Journal of Inflammation Research

Dovepress
Taylor & Francis Group

Open Access Full Text Article

ORIGINAL RESEARCH

Disruption of Gut Microbiota and Associated Fecal Metabolites in Collagen-Induced Arthritis Mice During the Early Stage

Dehong Wu[1,*], Mengdi Yin[2,*], Dandan Cao[2,*], Xiafeng Zhang[2], Yichun Zhu[2], Ying Wei[2], Yiling Li[2], Chengping Wen[2], Jia Zhou[2]

[1]Department of Rheumatology, The Second Affiliated Hospital of Zhejiang Chinese Medical University, Hangzhou, Zhejiang, 310005, People's Republic of China; [2]Institute of Basic Research in Clinical Medicine, College of Basic Medical Sciences, Zhejiang Chinese Medical University, Hangzhou, 310053, People's Republic of China

*These authors contributed equally to this work

Correspondence: Jia Zhou; Chengping Wen, Email zhoujia@zcmu.edu.cn; chengpw2010@126.com

Background: Rheumatoid arthritis (RA) is a chronic autoimmune disease and increasing evidence suggests that disturbances in the composition and function of gut microbiota are potentially implicated in the progression of RA. Further revealing the microbiota and related metabolic disorders in the preclinical stage of RA (pre-RA) is of great significance for exploration of disease mechanisms.

Methods: DBA/1 mice were injected with type II collagen on days 0 and 21 to establish collagen-induced arthritis (CIA) mouse model. Footpad thickness, serum autoantibodies, and joint histopathology were used to assess the progression of RA. A combination of 16S rRNA sequencing, untargeted metabolomics and targeted short-chain fatty acids (SCFAs) analysis were employed to comprehensively investigate the alterations of gut microbiota and fecal metabolites in CIA during the pre-RA stage.

Results: 20 days after the initial collagen immunization, CIA mice showed immune responses without joint symptoms, alongside gut microbiota disruption. Alterations were observed in 20 microbial taxa, including *Oscillospira, Bifidobacterium, Ruminococcus, Allobaculum, Alistipes, Lactobacillus, and Candidatus_Arthromitus*, etc. Untargeted and targeted metabolomics identified 33 altered fecal metabolites, mainly including sugars and their derivatives, amino acids, long-chain fatty acids and SCFAs, etc. Correlation analysis showed significant correlations between specific gut microbial abundances and fecal metabolite levels. Especially, SCFAs were strongly associated with *Bifidobacterium, Alistipes, Ruminococcus, Anaerotruncus*, and *Allobaculum*.

Conclusion: These findings suggest that collagen immunization leads to disruption of gut microbiome and induces changes of fecal metabolites in mice, which may play a key role in early development of RA in CIA mice.

Keywords: gut microbiota, fecal metabolites, short-chain fatty acids, preclinical stage, collagen-induced arthritis

Introduction

Rheumatoid arthritis (RA) is a chronic autoimmune disease that is characterized by inflammation of the synovium in peripheral joints. It is frequently accompanied by the involvement of organs outside of the joints, as well as the presence of inflammatory cytokines and autoantibodies in the serum. Before the onset of arthritis symptoms, patients may not fully meet the diagnostic criteria for RA. However, the immune system undergoes significant alterations, characterized by the activation of immune cells, and the production of autoantibodies, including anti-cyclic citrullinated peptide antibodies (anti-CCP) and rheumatoid factors (RF).[1] The preclinical stage of RA (pre-RA) is a crucial phase for exploring disease mechanisms,[1] so we focused on the pre-RA stage to investigate changes in disease manifestations and potential pathogenesis.

The etiology of RA is not fully understood, but it has been reported to have a strong correlation with environmental risk factors, genetic susceptibility, immune abnormalities, and other endogenous factors.[2] In recent years, numerous

Received: 28 October 2024
Accepted: 20 January 2025
Published: 4 February 2025

studies have highlighted the significant influence of gut microbiota in the development of RA. Dysbiosis of the gut microbiome is a prominent environmental factor that initiates RA, possibly by generating pro-inflammatory metabolites, compromising the integrity of the intestinal mucosal barrier, and inducing molecular mimicry of self-antigens, resulting in abnormal immune responses.[3–6] The combination of 16S rRNA sequencing and metabolomics technologies has been employed to explore the mechanisms underlying the development of various disease, such as depression, ischemic stroke, cancer.[7–9] Several studies have examining the alterations in gut microbiota and metabolites in RA patients. Certain gut microbiota and their associated metabolites have been found to have close associations with immune-mediated rheumatic diseases, such as RA, systemic lupus erythematosus, hyperuricemia, primary Sjogren's Syndrome.[6,10–13] For example, the abundance of Collinsella, which was increased/decreased in RA patients, has shown strong correlations with levels of β-alanine, as well as concentrations of α-amino adipic acid and tryptophanamide. Collinsella can increase the incidence and severity of arthritis and induce the expression of interleukin (IL)-17 cytokines.[6] However, there have been no studies to explore the gut microbiota and their associated metabolites with disorders in the early stage of RA by combining metagenomic and metabolomic approaches, which may be involved in the pathogenesis and progression of RA.

In order to reveal the characteristics of gut microbiome and fecal metabolome during the pre-RA stage and to investigate their respective contributions to the development of RA, we utilized techniques such as 16S rRNA gene sequencing, untargeted gas chromatography/mass spectrometry (GC/MS) metabolomics, and targeted short-chain fatty acid (SCFA) analysis to comprehensively explore the correlation between gut microbiota and fecal metabolites in a bovine type II collagen-induced arthritis (CIA) mouse model. The findings may provide new insights into the intrinsic mechanisms of gut microbiome's involvement in the development of RA.

Materials and Methods

Major Reagents and Chemicals

Bovine type II collagen, incomplete Freund's adjuvant (IFA), and complete Freund's adjuvant (CFA) were procured from Chondrex (Woodinville, Washington, USA). Methoxyamine, N-Methyl-N-(trimethylsilyl) trifluoroacetamide (MSTFA), and pyridine were obtained from Sigma-Aldrich (St. Louis, Missouri, USA). The SCFAs internal standard (2-ethylbutyric acid), was acquired from Yuan Ye (Shanghai, China). HPLC-grade acetonitrile, which served as the extraction solvent, was obtained from Merck (Fairfield, Ohio, USA). Ultra-pure water was supplied by the Milli-Q system (Millipore Corp., Millipore, MA, USA). The anti-CCP antibody Enzyme-Linked Immunosorbent Assay (ELISA) kit was obtained from CUSABIO (Wuhan, China).

Experimental Animals

Thirty specific pathogen-free (SPF)-grade male DBA/1 mice, aged 6–7 weeks, were obtained from Shanghai Slake Experimental Animal Co., Ltd. The weight of the DBA/1 mice used in this study was 16.47 g±0.22. The subjects were housed in a controlled SPF environment at the Experimental Animal Center of Zhejiang Chinese Medical University. The environment maintained a temperature of 25°C, relative humidity ranging from 40% to 60%, a 12-hour light-dark cycle, and provided the subjects with ad libitum access to food and water. The animal experiments were conducted in accordance with the Guidelines for the Care and Use of Laboratory Animals established by the US National Institutes of Health (NIH), and the animal research protocols have been approved by the Experimental Animal Health Ethics Committee of Zhejiang Chinese Medical University (IACUC-20220124-04).

Collagen Emulsion and CIA Induction

Preparation of Collagen Emulsion

To prepare the collagen solution, 10 mg of lyophilized bovine type II collagen powder was added to 5 mL of a 0.05 mol/L acetic acid solution. The mixture was gently stirred until well mixed, ensuring a final concentration of the collagen solution at 2 mg/mL. After storing at 4 °C overnight, the collagen solution was thoroughly mixed with an equal volume of complete Freund's adjuvant or incomplete Freund's adjuvant using a high-speed disperser to prepare an emulsion with a final concentration of 1 mg/mL, and the entire emulsification process was completed in an ice bath. The fully emulsified

emulsion was transferred to a 1 mL syringe which has been pre-cooled for primary immunization. Collagen emulsion prepared with complete Freund's adjuvant was transferred to a 1 mL syringe which has been pre-cooled for primary immunization, and collagen emulsion mixed with incomplete Freund's adjuvant for booster immunization.

CIA Modeling

On day 0, DBA/1 mice were injected intradermally into a vein at the base of the tail with 100 μL of bovine type II collagen solution prepared with complete Freund's adjuvant. On the 21st day, mice were injected subcutaneously into a dorsal vein with 100 μL of bovine type II collagen mixed with incomplete Freund's adjuvant to enhance their immune response. It was ensured that both injections were administered within a time frame of one hour.

Grouping

After one week of adaptive feeding, the mice were randomly allocated into two groups: the control group and the model group, each consisting of 15 mice. The model group was induced with CIA modeling. The control group received equal volumes of saline in the tail vein on days 0 and 21. On the 10th, 20th, and 42nd days, 5 control mice and 5 CIA mice, respectively, were executed and blood, fecal, and tissue samples were collected.

Evaluation of RA Progression

Measurement of Footpad Thickness

On the 0th day, a mark was placed on the hindfoot pads of the mice. The experimenter firmly grasped the mouse and accurately measured the thickness of the left hind pad using an electronic digital caliper with the mark as a reference point on the 10th, 20th, and 42nd days after the initial immunization. All measurements of pad thickness were conducted by the same researcher, who performed two measurements for each mouse.

Hematoxylin and Eosin (H&E) Staining

For histological evaluation, the hair and subcutaneous tissues were carefully excised from the affected joints in the lower limbs of the mice, while ensuring the preservation of the ankle joints. The joints were fixed in 4% paraformaldehyde, followed by decalcification in 10% EDTA. Subsequently, conventional dehydration was performed, and the tissues were embedded in paraffin. Paraffin blocks were then cut into sections with a thickness of 5 μm. Sections were stained with hematoxylin and eosin to assess the extent of tissue damage in the ankle joint.

Measurement of Serum Autoantibodies

Mice from each group were subjected to euthanasia on the 10th, 20th, and 42nd days after primary immunization. The blood sample was allowed to stand for duration of 2 h. Subsequently, centrifugation was performed at a speed of 3000 g for a period of 15 min in order to separate the serum from other components. The levels of anti-CCP antibodies in serum were quantified using an ELISA kit. Specific procedures were conducted in accordance with the instructions provided by the kit.

Analysis of Gut Microbiota

Feces were collected from the mice, and genomic DNA was extracted from the contents of each fecal sample using a OMEGA Soil DNA Kit. The DNA was extracted, and its molecular size was determined using 0.8% agarose gel electrophoresis. The DNA was quantified by ultraviolet spectrophotometer. In this experiment, the highly variable V3–V4 region of 16S rRNA gene of bacteria, using the forward primer 338F (5′-ACTCCTACGGGAGGCAGCA-3′) and the reverse primer 806R (5′-GGACTACHVGGGTWTCTAAT-3′), was selected for PCR amplification. The PCR products were quantified using a Microplate reader (BioTek, FLx800) with the Quant-iT PicoGreen dsDNA Assay Kit, and then combined based on the required amount of data for each sample. Use the TruSeq Nano DNA LT Library Prep Kit from Illumina to construct the database. For the qualified library, we used NovaSeq 6000 SP Reagent Kit (500 cycles) for 2 × 250bp double-terminal sequencing on the Illumina NovaSeq platform. The above operation was carried out by Shanghai Parkinson Biotechnology Co., Ltd.

https://doi.org/10.2147/JIR.S502980

Untargeted Analysis of Fecal Metabolome

20 mg of feces was mixed with a solution consisting of 500 μL of acetonitrile/water (v/v, 4/1). The mixture was then homogenized for 3 min at 30 hz using a cryo-ball mill (Retsch, Germany). After a 10-min period of settling, centrifugation was conducted at a temperature of 4°C and a speed of 12000 g for duration of 10 min. The supernatant (150 μL) was concentrated and dried utilizing the Labconco CentriVap system (Labconco, Kansas, Missouri, USA). Prior to GC/MS analysis, the freeze-dried metabolites were dissolved in a 50 μL solution of methoxyamine pyridine (20 mg/mL) and subjected to a reaction at 40°C for 90 min. After cooling, 40 μL of MSTFA was added for trimethylsilylation and allowed to react for 60 min. After derivatization, the resulting supernatant was carefully transferred into vials in order to facilitate subsequent analysis. In addition, 50 μL of supernatant was taken from each sample and mixed to prepare quality control (QC) samples, and the QC samples were processed in exactly the same way as the samples to be analyzed.

GC/MS analysis was conducted using an Agilent 7890/5975C GC/MS system (Agilent Technologies, Santa Clara, CA, USA). A 30 m × 0.25 mm × 0.25μm DB-5 MS fused quartz capillary column (J&W Scientific, Folsom, CA, USA) was utilized for separation. The injection volume of the sample was 1 μL, and it was split in a ratio of 10:1. Helium gas (99.999%) was employed as the carrier gas at a flow rate of 1.2 mL/min. The temperature program of the oven was set at 70°C for 3 min, followed by a ramp rate of 5°C/min until reaching 300°C, and then maintaining this temperature for a period of 15 min. The temperature of the injection port and the transfer line was adjusted to 280°C, while the EI ion source temperature was set to 220°C. Data was collected within the mass scan range of 33–600 amu following a solvent delay of 5 min. All samples were analyzed in a random order.

Measurement of Fecal SCFAs

The analysis of SCFAs in feces was conducted using the GC/MS method as described by Wen et al[14–16] A sample weighing 25 mg was taken and mixed with 500 μL of saturated NaCl solution. The mixture was then milled for 6 min at 30 hz using a cryogenic mixer mill (Retsch, Germany). Subsequently, 10 μL of 10% sulfuric acid was added to the sample and mixed for 30s using a vortex mixer (IKA Corporation). Then, 500 μL of ether (containing 2-ethylbutyric acid at a concentration of 8 μg/mL as an internal standard) was added for SCFAs extraction. The mixture was vortexed for 30s and then centrifuged at 12000 g for 15 min at 4°C. The ether supernatant was transferred to a 1.5 mL EP tube containing 0.25 g anhydrous sodium sulfate. Centrifugation was repeated under identical conditions to achieve dehydration, and subsequently, the solution was transferred to a GC sample bottle. Each individual sample was then injected onto a DB-WAX capillary column (30 m × 0.25 mm × 0.25μm) at a split ratio of 10:1, with 1 μL of sample being used for each injection. Helium gas was used as the carrier gas, maintaining a constant flow rate of 1.2 mL/min. The initial column temperature was set at 100°C and subsequently raised at a rate of 7.5°C/min until reaching 140°C. It was then further increased at a rate of 60°C/min until reaching 200°C, with a 3-min holding time. The temperature of the injection port was set to 240°C, the transfer line was set to 250°C, and the EI ion source was set to 230°C. The solvent delay time was set to 3.5 min, and the mass spectrometry acquisition range was configured to cover the m/z range of 40–400 amu.

Data Processing and Statistical Analysis

Gut microbiota: The sequencing raw data underwent analysis using the microbial ecology quantified insight QIIME2 (2019.4) software to identify high-quality reads. These reads were then clustered into Amplicon Sequence Variants (ASV). The qiime feature-table rarefy function was employed to rarefy the data, adjusting it to the sequencing depth equivalent to 95% of the minimum sample sequence count. This allowed for the examination of the ASVs and their respective relative abundance. By combining the Greengenes database[17] and the DADA2 classifier,[18] we achieved taxonomic identification of microbial sequences. Statistical analysis was conducted on the rarefied ASV table to determine the comprehensive composition of microbial communities at various taxonomic levels in each sample. Statistical analysis was conducted on the feature table after removing singletons. Non-parametric test was employed to determine the differences in bacterial abundance at the genus level between the model and the control groups during the pre-RA stage. The unrarefied ASV table was imported into R software to calculate alpha and beta diversity indices. Alpha diversity analysis was performed to assess Chao1, observed species, Shannon, Simpson, and Pielou's evenness

indices using non-parametric test in R software. For beta diversity analysis, unweighted UniFrac distance was calculated, and PERMANOVA test was used to analyze between-group differences through permutation (999 times). Principal coordinates analysis (PCoA) based on the distance matrix was conducted to visualize the difference between groups. To investigate the variations in microbial diversity among samples at a deeper level, we employed linear discriminant analysis effect size (LEfSe) method for conducting significance testing. A logarithmic LDA score of 2.0 was established as the threshold. Additionally, microbial functions were predicted by PICRUSt2 (phylogenetic investigation of communities by reconstruction of unobserved states 2)[19] upon MetaCyc (https://metacyc.org/) and KEGG (https://www.kegg.jp/) databases. To visualize the data, extended error bars were plotted using Stamp. Non-parametric test was employed to screen significantly different pathways between the control and CIA groups.

Untargeted fecal metabolome: the raw data of QC sample was imported into AMDIS 2.62 (NIST, Boulder, CO, USA) for deconvolution and peak recognition. This process resulted in the creation of a compound table that includes the retention time and quantitative ions for peak integration. Subsequently, MSD ChemStation (Agilent Technologies, Santa Clara, CA, USA) was utilized used to integrate all samples and generate a data matrix composed of retention time, quantitative ions, and corresponding areas for further statistical analysis. The data were normalized by dividing the area of each peak by the total area of all peaks in the corresponding sample, resulting in the relative intensity of each peak. The normalized data was imported into SIMCA-P V14.1 software (Umetrics AB, Umea, Sweden) for conducting multivariate statistical analysis. Principal component analysis (PCA) was performed to examine the metabolic alterations among the samples. This was followed by orthogonal partial least squares discriminant analysis (OPLS-DA) for the purpose of classifying CIA and control groups. Metabolites that exhibited significant changes between the CIA group and control group were screened based on the variable importance in projection (VIP) values of the OPLS-DA model (VIP>1) and non-parametric test conducted using SPSS 25.0 (International Business Machines Corp., Armonk, NY, USA) with a significance level ($P < 0.05$). After deconvolution of the peaks to eliminate the interference caused by overlapping peaks, the mass spectra of the metabolite peaks were compared with commercial mass spectrometry databases such as NIST and Wiley for structure identification using NIST14 software (National Institute of Standards and Technology, Gaithersburg, MD, USA). Metabolites exhibiting a similarity exceeding 80% were deemed as putative structures, and their identification was subsequently validated through the utilization of standard compounds.

Fecal SCFAs: Standard compounds were used for the identification of SCFAs. The MSD ChemStation software was utilized to integrate the respective peaks of all SCFAs in the samples. The data were normalized by employing internal standards, whereby the area of each peak was divided by the area of the internal standard peak in the corresponding sample. Non-parametric test (SPSS 25.0) was utilized to identify significantly altered SCFAs between the CIA group and control group. Statistical significance was defined as $P < 0.05$.

Spearman correlation was used to elucidate the association between the gut microbial community and perturbed metabolites. The correlation heatmap was visualized using Origin 2021 (9.8.0), while the correlation network was visualized using the Metware Cloud (https://cloud.metware.cn). When $P < 0.05$, the observed differences are deemed statistically significant.

Except for omics study, all other data were tested by nonparametric test to measure the statistical significance between the control and CIA groups using GraphPad Prism 8.0 (GraphPad Software, Inc.) software. The data are reported as the mean ± standard error (mean ± SE).

Results

Phenotypic Alterations in CIA Mice During the Pre-RA Stage

In this study, DBA/1 mice were used to establish a CIA model, and primary and booster immunizations with type II collagen were performed on the 0th and 21st days, respectively. During the experiment, there was no significant difference in body weight between the control and CIA groups (Figure S1). Anti-CCP antibodies are considered one of the key factors in synovial inflammation and damage in RA and may be detected even before the onset of arthritis symptoms. A significant elevation in serum levels of anti-CCP antibodies were observed in CIA mice on the 10th, 20th and 42nd days after primary immunization, compared to the control group (Figure 1A, $P<0.05$). By measuring the

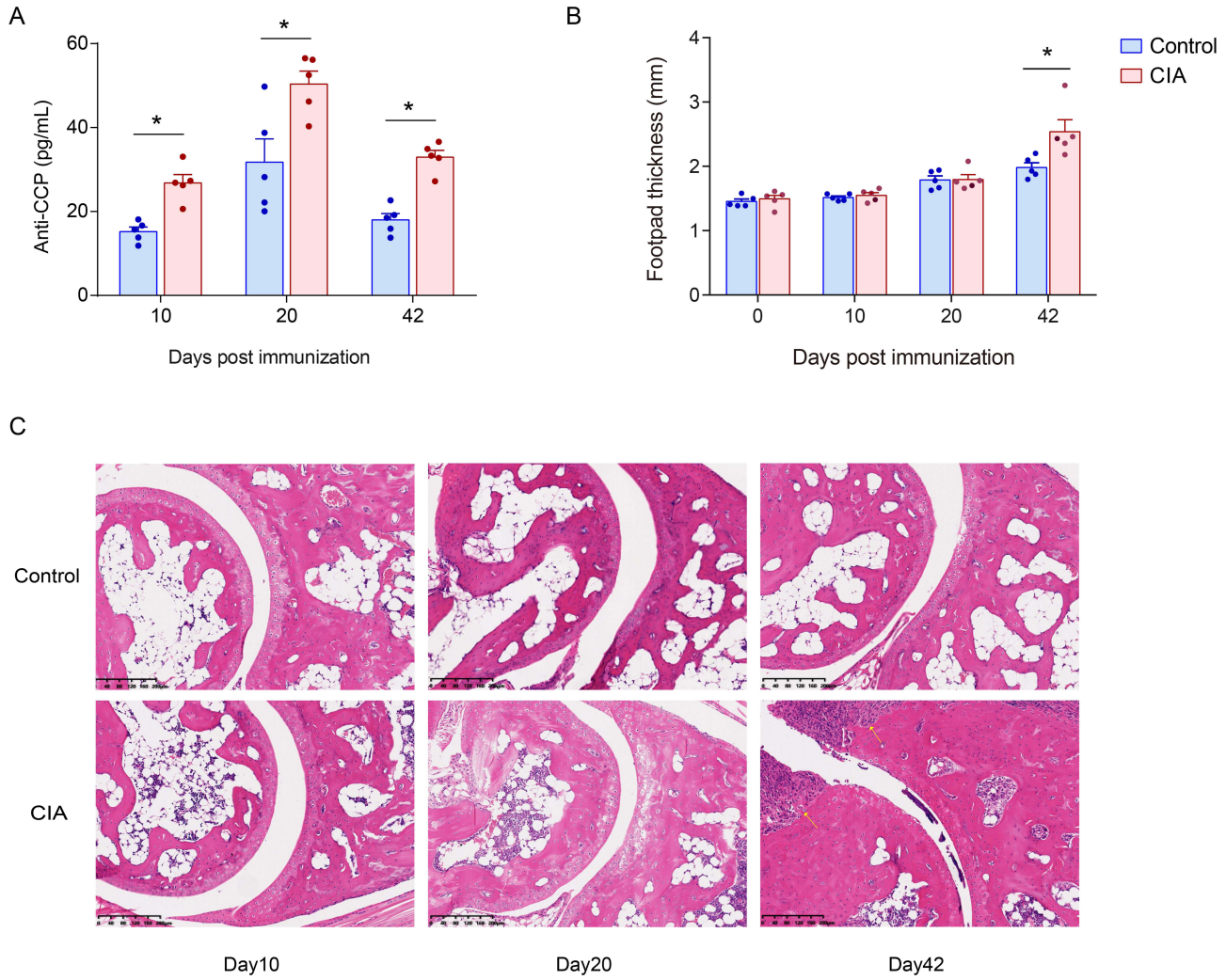

Figure 1 Differences in arthritis symptoms between control and CIA mice at different time points after immunization. (**A**) Serum level of anti-CCP antibodies, (**B**) footpad thickness, (**C**) representative images of H&E stained histology. * represents significantly different between the control and CIA groups (P<0.05).

thickness of footpads, the degree of joint inflammation and disease progression in CIA mice can be assessed. It was observed that the footpad thickness in the control group increased slightly with the increase of age; compared with the control group, the footpad thickness in the CIA group had no significant difference on the 10th and 20th days after the primary immunization, but increased greatly on the 42nd day, which was statistically significant (Figure 1B, P<0.05).

Furthermore, a histopathological analysis of the ankle joints was conducted using H&E staining, which demonstrated the absence of any pathological changes in the CIA mice on the 20th day, however, on the 42nd day, the mice in the CIA group exhibited erosion of joint cartilage (Figure 1C).

To sum up, DBA/1 mice developed an antigenic immune response after primary immunization, inducing the production of autoantibodies, such as anti-CCP antibodies; no joint symptoms were observed until 20 days following the injection of type II collagen. After booster immunization on the 21st day, CIA mice gradually developed joint inflammation, with a marked increase in footpad thickness and pathological damage by the 42nd day. Referring to the previous references, we regard the secondary immunization as the time division point between the pre-RA stage and the RA stage. Therefore, we collected the fecal samples of mice on the 20th day after the first immunization for flora and metabolite analysis. Referring to previous reference,[20] CIA mice on day 20 after collagen injection correspond to the early stage of RA.

Dysbiosis of Gut Microbiota in CIA Mice During the Pre-RA Stage

16S rRNA sequencing of the V3-V4 region of mouse feces were performed to reveal the changes in the gut microbiota of a CIA mouse model on the 20th day. The richness and diversity of the gut microbiota within the samples were assessed through alpha and beta diversity analysis. The Chao1 and Observed species indices in the model group showed a significant decrease compared to the control group on the 20th day, indicating a decrease in the richness of gut microbiota in the CIA group (Figure 2A, P<0.05). Additionally, the decline in Shannon and Simpson indices values suggests a reduction in the diversity of gut microbiota within the model group on the 20th day (Figure 2A, P=0.016, P=0.028. Pielou's evenness index is used to highlight the level of evenness within a community. In the CIA group, the evenness of gut microbiota decreased on the 20th day (Figure 2A, P<0.05). PCoA based on the beta diversity distances revealed differences in the composition of the microbial community between the two groups (Figure 2B). Examination of taxonomic data at the phylum level revealed a significant alteration in the relative abundance of *Proteobacteria, Deferribacteres*, and *Cyanobacteria* in the DBA/1 mice on the 20th day after primary immunization (Figure 2C, P<0.05).

To compare the microbial communities of fecal samples between the control and CIA groups on the 20th day, we conducted LEfSe analysis. The taxonomic branching diagram generated from the LEfSe sequence analysis is presented in Figure 3A. Based on effect size, we identified 4 taxonomic phyla that exhibited significant differences (LDA>2.0) at all taxonomic levels between the control and CIA groups. At the genus level, we observed 20 clusters that showed significant differences. Specifically, we observed a decrease in the genera of microbial taxa such as *Oscillospira, Haliangium, Bifidobacterium, Desulfovibrio, Mucispirillum, Ruminococcus, Parabacteroides, Allobaculum, Alistipes, Anaerotruncus*, and *Bilophila*. In contrast, the genera *Lactobacillus, Candidatus_Arthromitus, Thermoactinomyces, Rhodococcus, Delftia*, and *Acinetobacter* were enriched in the CIA group (Figure 3B).

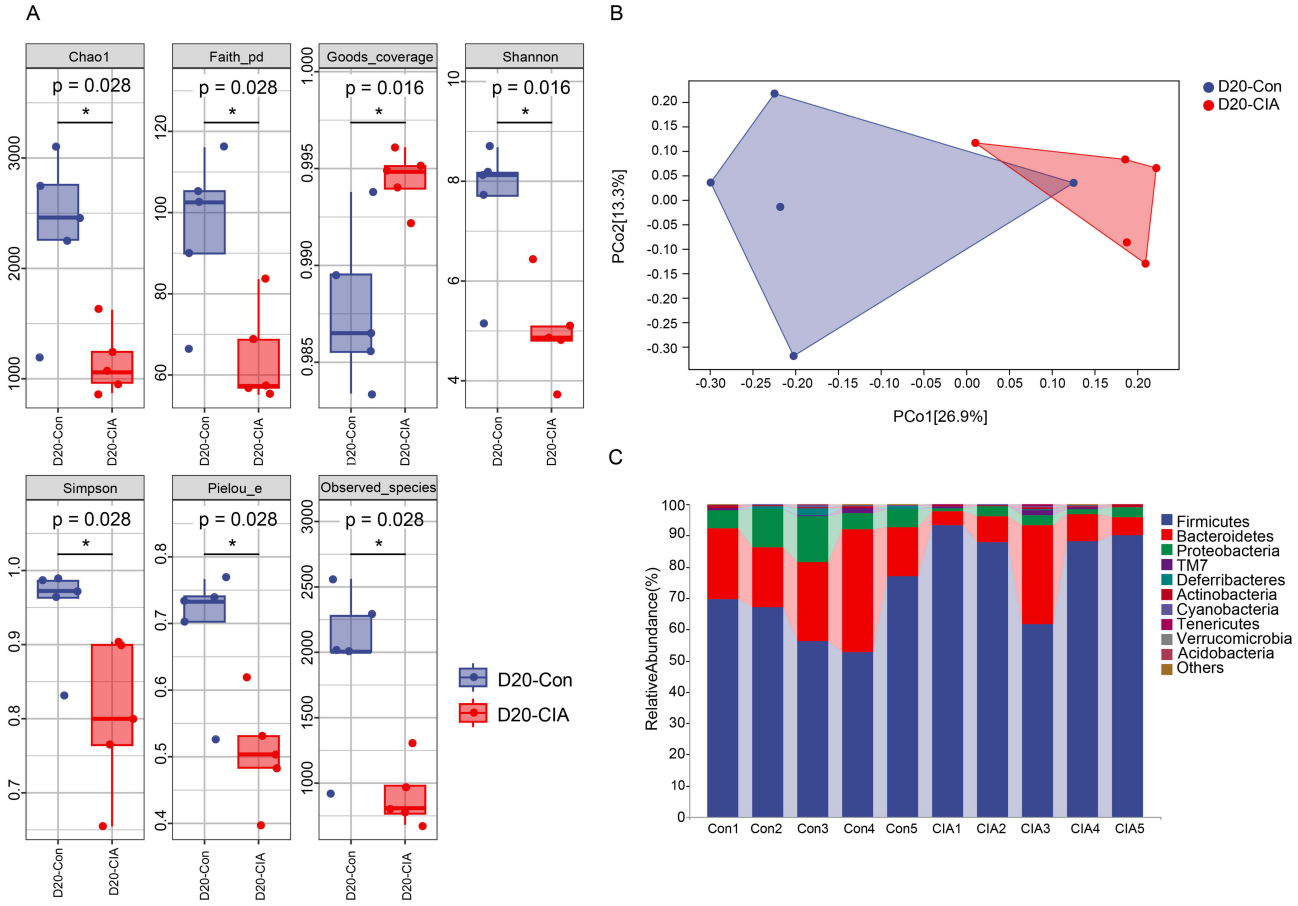

Figure 2 Differences in fecal microbiome between control and CIA mice during the pre-RA stage based on the 16S rRNA gene sequencing data. (**A**) Alpha diversity, (**B**) Beta diversity, and (**C**) compositional changes in the gut microbiome at the phylum level. * represents significantly different between the control and CIA groups (P<0.05).

https://doi.org/10.2147/JIR.S502980

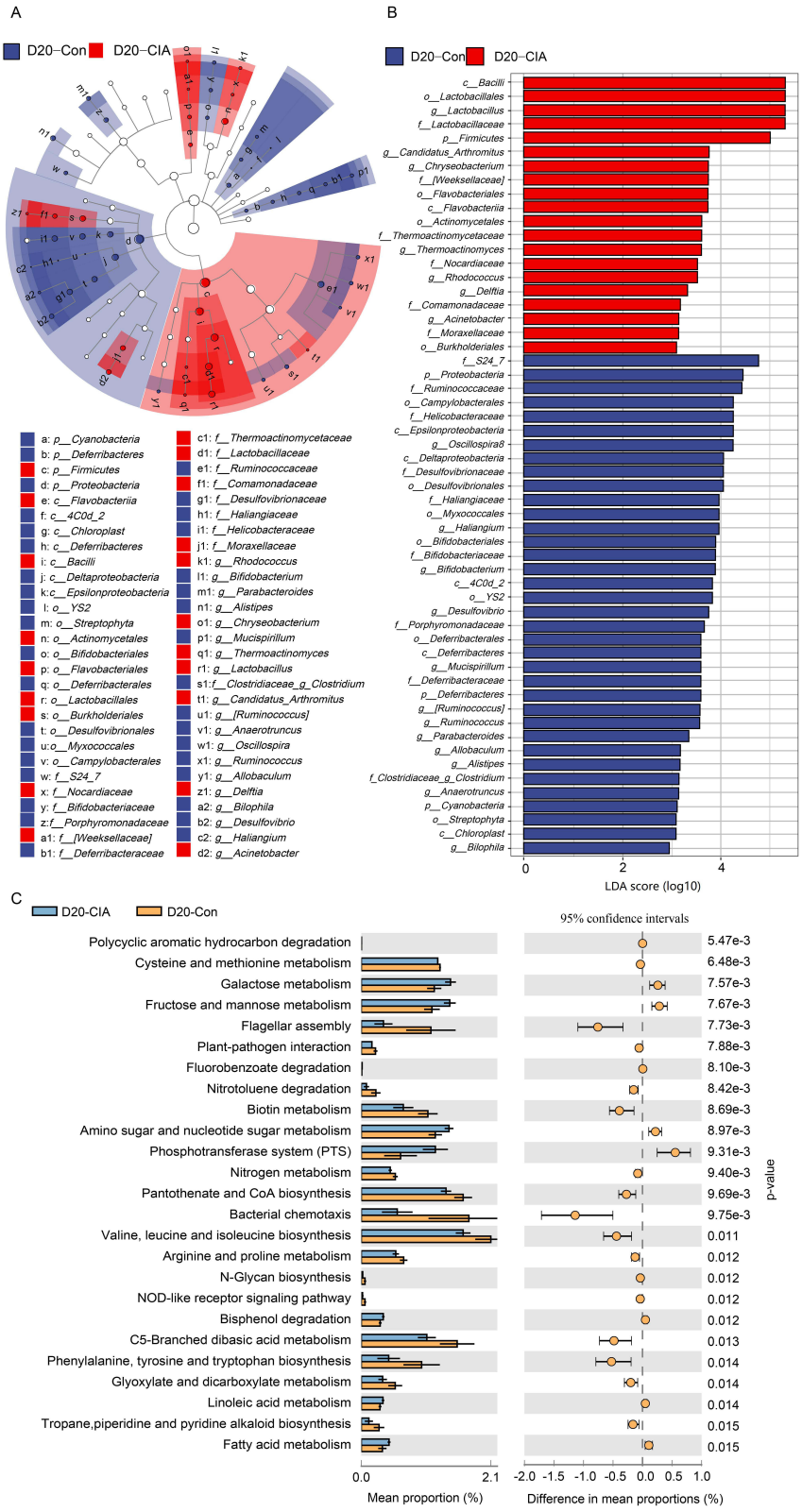

Figure 3 Differential fecal microbiota between control and CIA mice during the pre-RA stage. (**A**) Cladogram depicted significantly changed bacteria in the CIA group, as determined by LEfSe (LDA score >2 and P<0.05), (**B**) bar chart displaying different bacteria in the control and CIA groups, and (**C**) differential functional pathways of fecal microbiota between the two groups (top 25). The left panel displays a bar chart that reflects the average and standard error of each metabolic pathway. The bar chart illustrates variations in metabolic pathway between the two groups. The dot map represents the percentage change in the metabolic pathway at 95% confidence interval.

Furthermore, we utilized PICRUSt2 to predict changes in microbial functionality by comparing 16S rRNA gene sequencing data with microbial reference genome databases. Our findings indicate that alterations in the gut microbiota during the pre-RA state may impact various metabolic pathways. In total, we identified changes in 93 metabolic pathways (Figure 3C, Supplement Table 1). Specifically, carbohydrate metabolism was changed in CIA mice during the pre-RA stage, including galactose metabolism (P<0.01), fructose and mannose metabolism (P<0.01), amino sugar and nucleotide sugar metabolism (P<0.05), and glyoxylic acid and dicarboxylic acid metabolism (P<0.05). Additionally, we observed perturbations in amino acid metabolism and synthesis, such as cysteine and methionine metabolism (P<0.01), valine, leucine, and isoleucine biosynthesis (P<0.05), arginine and proline metabolism (P<0.05), and phenylalanine, tyrosine, and tryptophan biosynthesis (P<0.05); and lipid metabolism, including linoleic acid metabolism (P<0.05) and fatty acid metabolism (P<0.05).

Dysregulation of Fecal Microbiota Metabolism in CIA Mice During the Pre-RA Stage

In the present study, an untargeted metabolomics approach based on GC/MS technology was employed to analyze fecal samples obtained from mice on the 20th day. To depict the general distribution and clustering patterns of the control and CIA groups, PCA was performed on the metabolomics data. The resulting PCA score plot exhibited a separation between the CIA and control groups during the pre-RA stage, suggesting changes in mouse serum metabolism following the collagen injection (Figure 4A). OPLS-DA was employed to determine the altered fecal metabolites caused by collagen injection on the 20th day (Figure 4B–D). Differential metabolites were chosen based on their VIP values from the OPLS-DA model and P values from non-parametric test (VIP>1 and P<0.05). Finally, a total of 27 differential metabolites were identified in the study. These metabolites included various sugars and their derivatives such as 6-deoxymannose, fructose, galactose, mannose, arabinol, methylgalactoside, ribose, 2-deoxyribose, xylopyranose, inositol, and glucose-6-phosphate. Additionally, long-chain fatty acids such as heptadecanoate, hexadecanoate, pantothenate, linoleate, octadecanoate, and 5,8,11-eicosatrienoate were also changed in the fecal samples of CIA mice. Furthermore, amino acids including serine, glycine, tyrosine, aspartate, and cadaverine were found to be differential metabolites. Other metabolites such as urea, hypoxanthine, succinate, glycerate, and 2-aminobutyrate were also changed (Figure 4E, P<0.05).

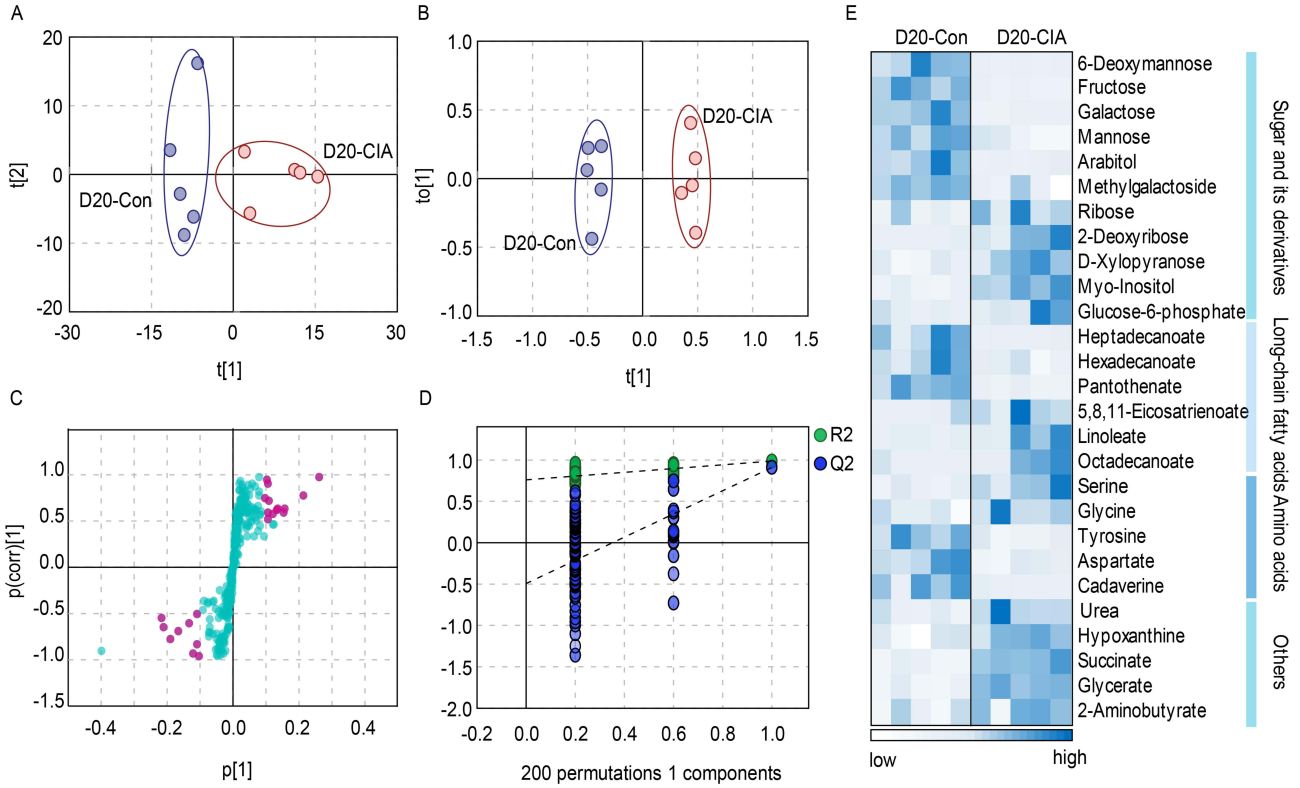

Figure 4 Differences in fecal metabolome between control and CIA mice during the pre-RA stage based on an untargeted metabolomics approach. (**A**) PCA score plot, (**B**) OPLS-DA score plot, (**C**) OPLS-DA S-plot, (**D**) OPLS-DA permutation test plot, (**E**) Heatmap of the altered fecal metabolites during the pre-RA stage (P<0.05).

https://doi.org/10.2147/JIR.S502980

Dysregulation of Fecal SCFAs in CIA Mice During the Pre-RA Stage

Previous studies have indicated that certain gut microbiota, such as *Bifidobacteriaceae, Parabacteroides, Alistipes, Ruminococcus, Anaerotruncus*, and *Allobaculum*, are associated with the production of SCFAs, particularly butanoate, acetate, and propionate.[21–24] Therefore, we employed a targeted metabolomics approach to examine the variations in SCFAs levels in fecal samples obtained from the CIA mice during the pre-RA stage. It is evident that the levels of 6 kinds of SCFAs, including acetate, propionate, isobutyrate, butanoate, 3-methyl-valerate, and valerate, exhibited a notable decrease in the feces of CIA mice on the 20th day after primary immunization (Figure 5, $P<0.05$). Regarding the potential implications of SCFAs in disease progression, we have conducted additional analysis to examine the levels of SCFAs on the 42nd day. The results indicated that the changes in multiple SCFAs observed on the 20th day, such as acetate, propionate, isobutyrate, 3-methyl-valerate, and valerate persisted through Day 42 (Figure 5, $P<0.05$).

Correlation of the Changed Microbiota and Metabolites in CIA Mice During the Pre-RA Stage

We performed Spearman correlation analysis to examine the relationship between microbial taxa and their contribution to the metabolites. Several metabolite levels exhibited significant correlations with bacterial abundance. Notably, a positive correlation was observed between *Lactobacillus* and linoleate as well as myo-Inositol, while a negative correlation was found with acetate. There existed a negative correlation between the abundance of *Bifidobacterium* and glycerate, while a positive correlation was observed with isobutyrate. In addition, *Myxococcales, [Weeksellaceae]*, and *Haliangium* showed positive correlations with tyrosine, 6-deoxymannose, and fructose, while displaying negative correlations with urea. *Flavobacteriia, Lactobacillales, Haliangiaceae*, and *Candidatus_Arthromitus* exhibited a negative correlation with isobutyrate, whereas *Bifidobacterium* and *[Weeksellaceae]* demonstrated a positive correlation. The following list presents the correlation relationships between the microbiota and metabolites (Figure 6A–F and Supplementary Table 2).

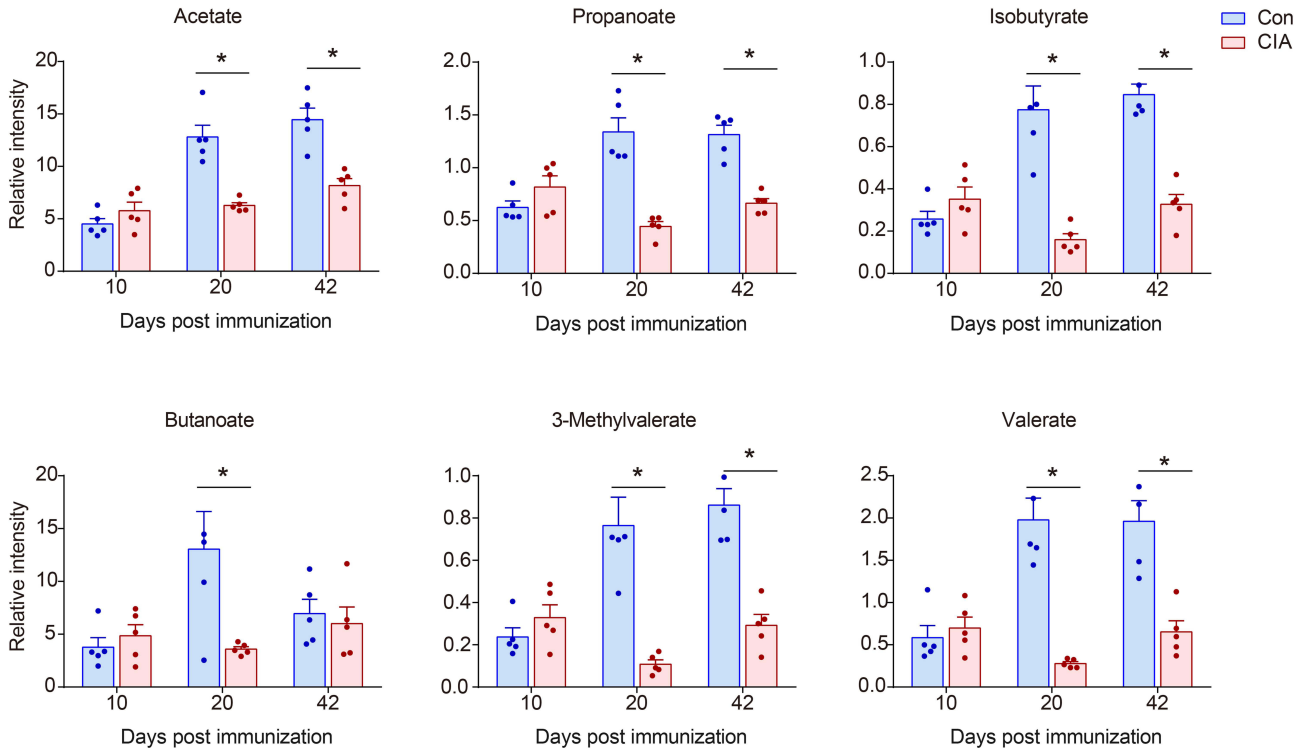

Figure 5 Differences in fecal SCFAs between control and CIA mice at different time points after immunization based on a targeted metabolomics approach. * represents significantly different between the control and CIA groups ($P<0.05$).

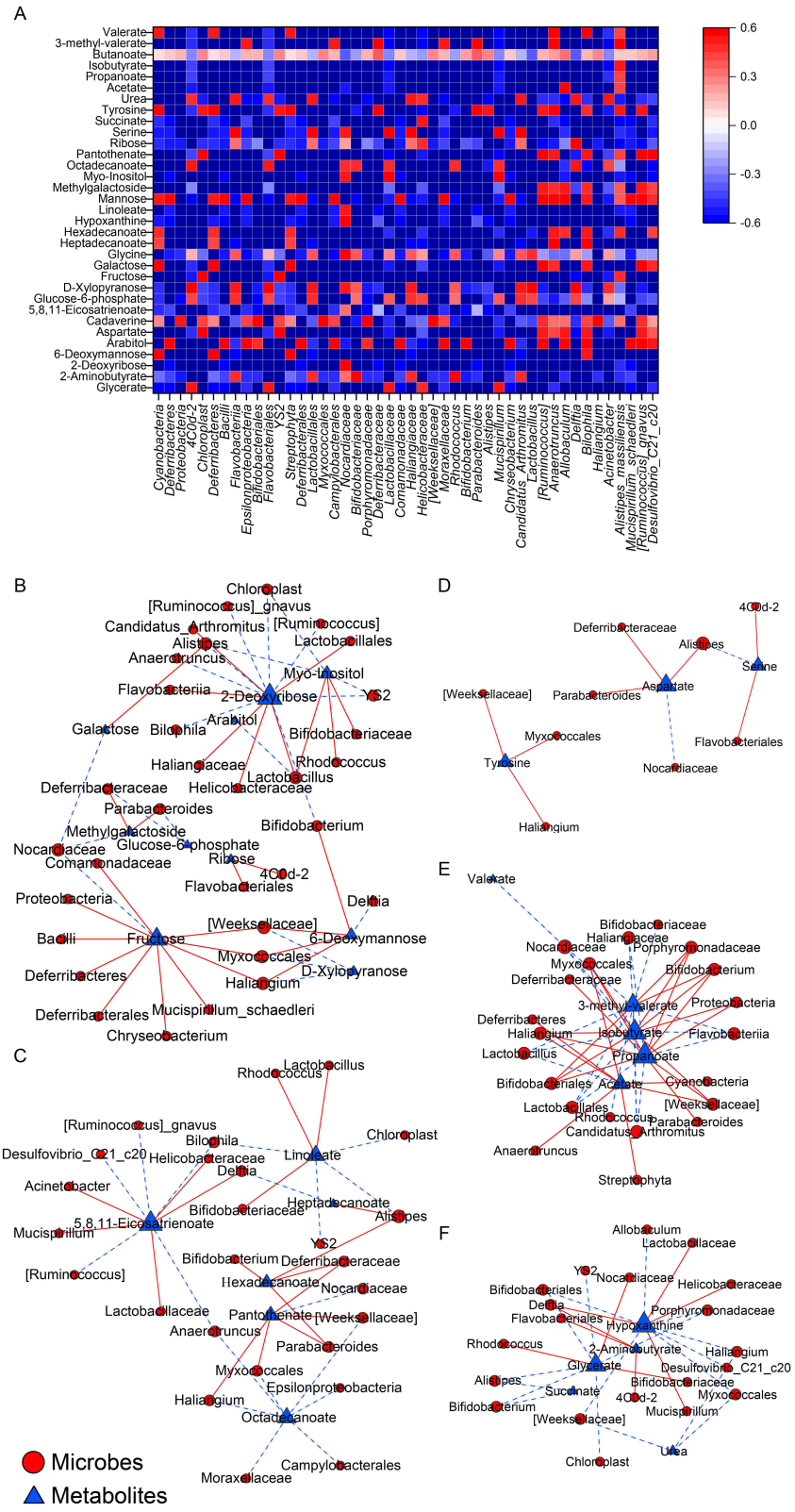

Figure 6 Spearman correlation between the gut microbiota and fecal metabolites in CIA mice during the pre-RA stage. (**A**) Heatmap of correlation coefficients. Red squares represent positive correlation, blue squares represent negative correlation, white squares represent no correlation. Network diagram of the correlations between microbes and fecal metabolites. Fecal metabolites include (**B**) sugars and their derivatives, (**C**) long-chain fatty acids, (**D**) amino acids, (**E**) SCFAs, and (**F**) others. Red solid lines represent positive correlation between microbes and metabolites, blue dashed lines represent negative correlation(|r|> 0.8).

https://doi.org/10.2147/JIR.S502980

Discussion

In this study, DBA/1 mice were injected with type II collagen on days 0 and 21 to establish CIA model. Prior to booster immunization on the 21st day, the CIA group developed an antigenic immune response without joint symptoms. Therefore, as in the literature,[25] Day 20 was identified as the time point to delineate the pre-RA stage from the RA stage. We employed 16S rRNA sequencing, targeted and untargeted metabolomics to investigate the alterations in the gut microbiota and metabolome in fecal samples at the pre-RA stage. It was observed that CIA mice have exhibited dysbiosis of gut microbiota and disruption of microbial metabolism at the pre-RA stage. Specifically, there was a decrease in the abundance of *Bifidobacterium, Parabacteroides, Alistipes, Ruminococcus, Anaerotruncus, Allobaculum*, etc., while there was an increase in the abundance of *Lactobacillus*, etc. This was accompanied by typical alterations in the concentrations of several microbial metabolites, including linoleate, acetate, glycerate, tyrosine, urea, fructose, and isobutyrate, etc.

Increasing evidence suggests that disturbances in the composition and function of gut microbiota are implicated in the pathogenesis of RA, and in the present study, a decrease in alpha diversity and an alteration in beta diversity of gut flora were observed in the CIA group at the pre-RA stage. Lactobacillus can stimulate Th17 activity and inhibit Treg activity, inducing RA in germ-free animals, which is increased in both RA patients and models.[26–29] *Candidatus_Arthromitus* also induced the differentiation of Th17 cells and promoted intestinal inflammation.[30,31] We found that the abundance of Lactobacillus increased at the pre-RA stage of CIA mice, which may disrupt the balance of Th17/Treg and promote the disease progression in CIA mice. *Allobaculum* is able to exacerbate colonic inflammation and elicit antigen-specific mucosal responses.[32,33] *Mucispirillum* accumulates predominantly in the intestinal mucus layer and acts as mucin degraders, which are involved in intestinal inflammation.[34–37] *Ruminococcus_gnavus* is positively associated with the loss of the epithelial barrier, which leads to mucus degradation, intestinal barrier instability, and low-grade mucosal inflammation.[38,39] As harmful bacteria in gastrointestinal tract, *Desulfovibrio* can produce hydrogen sulfide which is toxic to intestinal epithelial cells. Several clinical studies have confirmed the increased abundance of *Desulfovibrio spp*. as an important feature of ulcerative colitis disease.[40,41] The decrease in the abundance of the above four genera at the pre-RA stage of CIA mice suggests that inflammatory colitis may not yet occurred in CIA mice at this stage.

Bioactive metabolites such as SCFAs, polysaccharides, polyamines, bile acids, produced by intestinal flora are mediators of microbial-host communication and are essential for the maintenance of host physiological functions. Intestinal homeostasis imbalance is closely related to the development of metabolic, immune and other systemic diseases. Therefore, exploring the alterations in fecal metabolites can provide new insights into the pathological mechanism of RA. SCFAs are extremely important anti-inflammatory metabolites in the gut and have a protective effect on the intestinal barrier. Exogenously ingested dietary cellulose is fermented and decomposed into SCFAs by specific gut microbiota, of which the three most highly abundant SCFAs are acetate, propionate, and butanoate. We found that acetate, propionate and butanoate were significantly reduced in the feces of CIA mice during the pre-RA stage. *Alistipes* is a producer of acetate and propionate,[21] so a decrease in *Alistipes* at the pre-RA stage in CIA mice may lead to a decrease of acetate (r=0.697) and propionate (r=0.721), and there was a significant correlation between *Alistipes* and SCFAs. *Anaerotruncus, Ruminococcus, Bifidobacterium* and *Parabacteroides* are also bacterial sources of acetate,[22–24] and the reduction of these bacteria may further contribute to lower acetate level (r=0.828, r=0.745, r=0.681, r=0.758). *Allobaculum* belongs to Phylum *Firmicutes*, can yield butanoate from carbohydrates.[32,42,43] We found that CIA mice showed a decrease in *Allobaculum* abundance and butanoate level at the pre-RA stage. Therefore, we speculate that the changes of the above gut microbes may promote the inflammatory response of RA by affecting the abundance of SCFAs.

Our untargeted metabolomics data revealed alterations in a variety of amino acids during the pre-RA stage in feces of CIA mice, such as an increase in glycine and serine, and a decrease in tyrosine and aspartate. Aspartate is closely associated with RA, and a deficiency in mitochondrial aspartate can result in the production of transmembrane TNF in T cells, thereby exacerbating synovial inflammation.[44] Tyrosine is a kind of aromatic amino acids, the microbe-derived metabolites from aromatic amino acids have an ameliorating role in regulating intestinal barrier function.[45] Intestinal amino acids such as glycine and serine can serve as precursors for the synthesis of SCFAs by anaerobic bacteria thus playing a role in the development of RA.[46] Underutilization can lead to the accumulation of the above amino acids in feces and promote a shift from anti-inflammatory to pro-inflammatory state during the development of RA. Cadaverine is

primarily synthesized through the decarboxylation of amino acids by microorganisms, such as *Bifidobacterium, Lactobacilli* and *Streptococcus*.[47] We found that both *Bifidobacterium* abundance and cadaverine levels were significantly decreased and there was a significant correlation between them (r=0.658).

In the intestine, succinate can be produced by bacteria such as *Alistipes*, and *Parabacteroides* (r=−0.842, r=−0.636).[48,49] In addition to the crucial role in mitochondrial ATP production, succinate also serves as an important pro-inflammatory metabolite that has the potential to induce and maintain a pro-inflammatory state in macrophages, leading to chronic inflammation.[50] Elevated levels of fecal succinate at the pre-RA stage may trigger inflammatory state in CIA mice. Linoleate and 5, 8, 11-eicosatrienoate are important polyunsaturated fatty acids with significant antioxidant and anti-inflammatory properties.[51] Elevated levels of polyunsaturated fatty acids in CIA mice may exert a potent anti-inflammatory effect to mitigate the development of RA. An insufficiency of probiotics containing urease, such as *Bifidobacterium* (r=−0.644), or an excessive presence of pathogenic bacteria without detoxification capabilities, may result in elevated levels of urea.[52] In addition, hypoxanthine and glucose-6-phosphate, which appear elevated in the feces of CIA mice during the pre-RA stage, have also been found to be elevated in the serum of patients[53] and CIA rats[54] during the RA stage.

Conclusion

In the study, 16S rRNA gene sequencing, untargeted GC/MS metabolomics, and targeted SCFAs analysis were combined to explore the alterations in gut microbiota and fecal metabolome in collagen-induced arthritis mice at the early stage of RA. The results showed that CIA mice have exhibited reduced bacterial diversity and abnormal fecal metabolome during the pre-RA stage. Correlation analysis revealed a close interaction between specific gut microbiota and fecal metabolites. In particular, the levels of SCFAs are strongly associated with the abundances of various bacteria such as *Bifidobacterium, Alistipes, Ruminococcus, Anaerotruncus*, and *Allobaculum*. The findings of the research provide a novel perspective, indicating that the disturbance of gut microbiome and metabolome may play a key role in the early stage of RA, which could help to further investigate the specific roles of microorganisms and key metabolites in the pathogenesis of RA.

Acknowledgments

We appreciate the technical support from the Public Platform of Medical Research Center, Academy of Chinese Medical Science, Zhejiang Chinese Medical University.

Funding

This study was supported by the Bureau and Provincial Joint Construction of Science and Technology Plan Project (NO. GZY-ZJ-KJ-23009), the National Natural Science Foundation of China (NO. 81873102), and the Zhejiang Provincial Natural Science Foundation of China (NOS. LY22H290006 and LBY22H270003).

Disclosure

No potential conflict of interest was reported by the authors.

References

1. Meehan GR, Thomas R, Al Khabouri S, et al. Preclinical models of arthritis for studying immunotherapy and immune tolerance. *Ann Rheum Dis*. 2021;80:1268–1277. doi:10.1136/annrheumdis-2021-220043
2. Petrovská N, Prajzlerová K, Vencovský J, et al. The pre-clinical phase of rheumatoid arthritis: from risk factors to prevention of arthritis. *Autoimmun Rev*. 2021;20:102797. doi:10.1016/j.autrev.2021.102797
3. Kau AL, Ahern PP, Griffin NW, et al. Human nutrition, the gut microbiome and the immune system. *Nature*. 2011;474:327–336. doi:10.1038/nature10213
4. Zhao T, Wei Y, Zhu Y, et al. Gut microbiota and rheumatoid arthritis: from pathogenesis to novel therapeutic opportunities. *Front Immunol*. 2022;13:1007165. doi:10.3389/fimmu.2022.1007165
5. Yu D, Du J, Pu X, et al. The gut microbiome and metabolites are altered and interrelated in patients with rheumatoid arthritis. *Front Cell Infect Microbiol*. 2021;11:763507. doi:10.3389/fcimb.2021.763507

6. Chen J, Wright K, Davis JM, et al. An expansion of rare lineage intestinal microbes characterizes rheumatoid arthritis. *Genome Med*. 2016;8:43. doi:10.1186/s13073-016-0299-7
7. Yu M, Jia H, Zhou C, et al. Variations in gut microbiota and fecal metabolic phenotype associated with depression by 16S rRNA gene sequencing and LC/MS-based metabolomics. *J Pharm Biomed Anal*. 2017;138:231–239. doi:10.1016/j.jpba.2017.02.008
8. Zhao L, Wang C, Peng S, et al. Pivotal interplays between fecal metabolome and gut microbiome reveal functional signatures in cerebral ischemic stroke. *J Transl Med*. 2022;20:459. doi:10.1186/s12967-022-03669-0
9. Zhu Z, Cai J, Hou W, et al. Microbiome and spatially resolved metabolomics analysis reveal the anticancer role of gut akkermansia muciniphila by crosstalk with intratumoral microbiota and reprogramming tumoral metabolism in mice. *Gut Microbes*. 2023;15:2166700. doi:10.1080/19490976.2023.2166700
10. Choi SC, Brown J, Gong M, et al. Gut microbiota dysbiosis and altered tryptophan catabolism contribute to autoimmunity in lupus-susceptible mice. *Sci Transl Med*. 2020:12. doi:10.1126/scitranslmed.aax2220
11. Zhang L, Qing P, Yang H, et al. Gut microbiome and metabolites in systemic lupus erythematosus: link, mechanisms and intervention. *Front Immunol*. 2021;12:686501. doi:10.3389/fimmu.2021.686501
12. Song S, Lou Y, Mao Y, et al. Alteration of gut microbiome and correlated amino acid metabolism contribute to hyperuricemia and Th17-driven inflammation in Uox-KO mice. *Front Immunol*. 2022;13:804306. doi:10.3389/fimmu.2022.804306
13. Yang L, Xiang Z, Zou J, et al. Comprehensive analysis of the relationships between the gut microbiota and fecal metabolome in individuals with primary sjogren's syndrome by 16S rRNA sequencing and LC-MS-based metabolomics. *Front Immunol*. 2022;13:874021. doi:10.3389/fimmu.2022.874021
14. Wen X, Lou Y, Song S, et al. Qu-Zhuo-Tong-Bi decoction alleviates gouty arthritis by regulating butyrate-producing bacteria in mice. *Front Pharmacol*. 2020;11:610556. doi:10.3389/fphar.2020.610556
15. Zhang S, Wang H, Zhu MJ. A sensitive GC/MS detection method for analyzing microbial metabolites short chain fatty acids in fecal and serum samples. *Talanta*. 2019;196:249–254. doi:10.1016/j.talanta.2018.12.049
16. Li X, Gui R, Wang X, et al. Oligosaccharides isolated from rehmannia glutinosa protect LPS-induced intestinal inflammation and barrier injury in mice. *Front Nutr*. 2023;10:1139006. doi:10.3389/fnut.2023.1139006
17. DeSantis TZ, Hugenholtz P, Larsen N, et al. Greengenes, a chimera-checked 16S rRNA gene database and workbench compatible with ARB. *Appl Environ Microbiol*. 2006;72:5069–5072. doi:10.1128/aem.03006-05
18. Callahan BJ, McMurdie PJ, Rosen MJ, et al. DADA2: high-resolution sample inference from illumina amplicon data. *Nat Methods*. 2016;13(7):581–583. doi:10.1038/nmeth.3869
19. Douglas GM, Maffei VJ, Zaneveld JR, et al. PICRUSt2 for prediction of metagenome functions. *Nat Biotechnol*. 2020;38:685–688. doi:10.1038/s41587-020-0548-6
20. Xue M, Dervish S, McKelvey KJ, et al. Activated protein C targets immune cells and rheumatoid synovial fibroblasts to prevent inflammatory arthritis in mice. *Rheumatology*. 2019;58:1850–1860. doi:10.1093/rheumatology/key429
21. Rau M, Rehman A, Dittrich M, et al. Fecal SCFAs and SCFA-producing bacteria in gut microbiome of human NAFLD as a putative link to systemic T-cell activation and advanced disease. *United European Gastroenterol J*. 2018;6:1496–507. doi:10.1177/2050640618804444
22. Lawson PA, Song Y, Liu C, et al. Anaerotruncus colihominis gen. nov., sp. nov., from human faeces. *Int J Syst Evol Microbiol*. 2004;54:(Pt 2) 413–417. doi:10.1099/ijs.0.02653-0
23. Russell WR, Hoyles L, Flint HJ, et al. Colonic bacterial metabolites and human health. *Curr Opin Microbiol*. 2013;16:246–54. doi:10.1016/j.mib.2013.07.002
24. Sakamoto M, Benno Y. Reclassification of bacteroides distasonis, bacteroides goldsteinii and bacteroides merdae as parabacteroides distasonis gen. nov. comb. nov. parabacteroides goldsteinii comb. nov. and parabacteroides merdae comb. nov. *Int J Syst Evol Microbiol*. 2006;56:1599–1605. doi:10.1099/ijs.0.64192-0
25. Han Z, Boyle DL, Manning AM, et al. AP-1 and NF-kappaB regulation in rheumatoid arthritis and murine collagen-induced arthritis. *Autoimmunity*. 1998;28:197–208. doi:10.3109/08916939808995367
26. Lee JY, Mannaa M, Kim Y, et al. Comparative analysis of fecal microbiota composition between rheumatoid arthritis and osteoarthritis patients. *Genes*. 2019;11:10. doi:10.3390/genes10100748
27. Scher JU, Abramson SB. The microbiome and rheumatoid arthritis. *Nat Rev Rheumatol*. 2011;7:569–578. doi:10.1038/nrrheum.2011.121
28. Liu X, Zou Q, Zeng B, et al. Analysis of fecal lactobacillus community structure in patients with early rheumatoid arthritis. *Curr Microbiol*. 2013;67(2):170–176. doi:10.1007/s00284-013-0338-1
29. Kano H, Kaneko T, Kaminogawa S. Oral intake of lactobacillus delbrueckii subsp. bulgaricus OLL1073R-1 prevents collagen-induced arthritis in mice. *J Food Prot*. 2002;65(1):153–160. doi:10.4315/0362-028x-65.1.153
30. Flannigan KL, Denning TL. Segmented filamentous bacteria-induced immune responses: a balancing act between host protection and autoimmunity. *Immunology*. 2018;154:537–546. doi:10.1111/imm.12950
31. Morgan XC, Tickle TL, Sokol H, et al. Dysfunction of the intestinal microbiome in inflammatory bowel disease and treatment. *Genome Biol*. 2012;13:R79. doi:10.1186/gb-2012-13-9-r79
32. Balakrishnan B, Luckey D, Bodhke R, et al. Prevotella histicola protects from arthritis by expansion of allobaculum and augmenting butyrate production in humanized Mice. *Front Immunol*. 2021;12:609644. doi:10.3389/fimmu.2021.609644
33. Rice TA, Bielecka AA, Nguyen MT, et al. Interspecies commensal interactions have nonlinear impacts on host immunity. *Cell Host Microbe*. 2022;30:988–1002e6. doi:10.1016/j.chom.2022.05.004
34. Xiao M, Fu X, Ni Y, et al. Protective effects of paederia scandens extract on rheumatoid arthritis mouse model by modulating gut microbiota. *J Ethnopharmacol*. 2018;226:97–104. doi:10.1016/j.jep.2018.08.012
35. Berry D, Schwab C, Milinovich G, et al. Phylotype-level 16S rRNA analysis reveals new bacterial indicators of health state in acute murine colitis. *ISME J*. 2012;6:2091–2106. doi:10.1038/ismej.2012.39
36. El Aidy S, Derrien M, Aardema R, et al. Transient inflammatory-like state and microbial dysbiosis are pivotal in establishment of mucosal homeostasis during colonisation of germ-free mice. *Benef Microbes*. 2014;5:67–77. doi:10.3920/bm2013.0018
37. Berry D, Kuzyk O, Rauch I, et al. Intestinal microbiota signatures associated with inflammation history in mice experiencing recurring colitis. *Front Microbiol*. 2015;6:1408. doi:10.3389/fmicb.2015.01408

38. Henke MT, Kenny DJ, Cassilly CD, et al. Ruminococcus gnavus, a member of the human gut microbiome associated with Crohn's disease, produces an inflammatory polysaccharide. *Proc Natl Acad Sci U S A*. 2019;116:12672–12677. doi:10.1073/pnas.1904099116
39. Breban M, Tap J, Leboime A, et al. Faecal microbiota study reveals specific dysbiosis in spondyloarthritis. *Ann Rheum Dis*. 2017;76:1614–1622. doi:10.1136/annrheumdis-2016-211064
40. Verstreken I, Laleman W, Wauters G, et al. Desulfovibrio desulfuricans bacteremia in an immunocompromised host with a liver graft and ulcerative colitis. *J Clin Microbiol*. 2012;50:199–201. doi:10.1128/jcm.00987-11
41. Chen YR, Jing QL, Chen FL, et al. Desulfovibrio is not always associated with adverse health effects in the Guangdong gut microbiome project. *PeerJ*. 2021;9:e12033. doi:10.7717/peerj.12033
42. Konikoff T, Gophna U. Oscillospira: a central, enigmatic component of the human gut microbiota. *Trends Microbiol*. 2016;24:523–524. doi:10.1016/j.tim.2016.02.015
43. Zhou W, Yang T, Xu W, et al. The polysaccharides from the fruits of Lycium barbarum L. confer anti-diabetic effect by regulating gut microbiota and intestinal barrier. *Carbohydr Polym*. 2022;291:119626. doi:10.1016/j.carbpol.2022.119626
44. Wu B, Zhao TV, Jin K, et al. Mitochondrial aspartate regulates TNF biogenesis and autoimmune tissue inflammation. *Nat Immunol*. 2021;22:1551–1562. doi:10.1038/s41590-021-01065-2
45. Li J, Zhang L, Wu T, et al. Indole-3-propionic acid improved the intestinal barrier by enhancing epithelial barrier and mucus barrier. *J Agric Food Chem*. 2021;69:1487–1495. doi:10.1021/acs.jafc.0c05205
46. Neis EP, Dejong CH, Rensen SS. The role of microbial amino acid metabolism in host metabolism. *Nutrients*. 2015;7:2930–2946. doi:10.3390/nu7042930
47. Pi Y, Gao K, Zhu W. Advances in host-microbe metabolic axis. *Wei Sheng Wu Xue Bao*. 2017;57:161–169.
48. Fernández-Veledo S, Vendrell J. Gut microbiota-derived succinate: friend or foe in human metabolic diseases? *Rev Endocr Metab Disord*. 2019;20:439–447. doi:10.1007/s11154-019-09513-z
49. Wang K, Liao M, Zhou N, et al. Parabacteroides distasonis alleviates obesity and metabolic dysfunctions via production of succinate and secondary bile acids. *Cell Rep*. 2019;26:222–35e5. doi:10.1016/j.celrep.2018.12.028
50. Mills E, O'Neill LA. Succinate: a metabolic signal in inflammation. *Trends Cell Biol*. 2014;24:313–320. doi:10.1016/j.tcb.2013.11.008
51. Hsu LC, Wen ZH, Chen HM, et al. Evaluation of the anti-inflammatory activities of 5, 8, 11-cis-Eicosatrienoic acid. *Food and Nutrition Sciences*. 2013;4:36478. doi:10.4236/fns.2013.49A1018
52. Chen H, Tong T, Lu SY, et al. Urea cycle activation triggered by host-microbiota maladaptation driving colorectal tumorigenesis. *Cell Metab*. 2023;35:651–66e7. doi:10.1016/j.cmet.2023.03.003
53. Madsen RK, Lundstedt T, Gabrielsson J, et al. Diagnostic properties of metabolic perturbations in rheumatoid arthritis. *Arthritis Res Ther*. 2011;13:R19. doi:10.1186/ar3243
54. Li Z, Nie L, Li Y, et al. Traditional Tibetan medicine twenty-five wei'er tea pills ameliorate rheumatoid arthritis based on chemical crosstalk between gut microbiota and the host. *Front Pharmacol*. 2022;13:828920. doi:10.3389/fphar.2022.828920